

Dynamics of photoinduced change of magnetoanisotropy parameter in orthoferrites probed with terahertz excited coherent spin precession

Keita Yamaguchi,^{1,*} Takayuki Kurihara,¹ Hiroshi Watanabe,¹ Makoto Nakajima,² and Tohru Suemoto¹¹*Institute for Solid State Physics, The University of Tokyo, Kashiwa, Chiba 277-8581, Japan*²*Institute of Laser Engineering, Osaka University, Suita, Osaka 565-0871, Japan*

(Received 12 December 2014; revised manuscript received 5 June 2015; published 3 August 2015)

The effects of femtosecond laser excitation on the anisotropy parameter in orthoferrites ErFeO_3 and DyFeO_3 were probed through Faraday rotation induced by coherent spin precession, which was triggered by a terahertz pulse. Through the delayed frequency shift of the precession, gradual change in the anisotropic energy of the iron spins is evidenced. This is attributed to the slow energy transfer from the Fe^{3+} $3d$ electron system to the rare-earth $4f$ electron system, which in turn alters the anisotropy parameter of the Fe^{3+} spins. The result presented here reveals the time dependent spin alignment mechanism in cant-type antiferromagnetic orthoferrites and enables deeper understanding of spin orientation dynamics triggered by electronic excitation.

DOI: [10.1103/PhysRevB.92.064404](https://doi.org/10.1103/PhysRevB.92.064404)

PACS number(s): 75.78.Jp, 76.50.+g, 78.20.Ls

Exploitation of the spin degrees of freedom in an ultrafast regime is a research field which is receiving intense attention. Motivated by the rapid progress in the femtosecond laser spectroscopy, ultrafast optical excitation of the spins has been developed. Because this technique enables subpicosecond time scale spin manipulation [1–9], it is highly promising for development of unprecedentedly fast optical memory, spintronics, and quantum computing.

Numbers of intriguing works on femtosecond spin excitation have been reported in the past [1–5]. These works show various important results on spin ordering dynamics such as femtosecond antiferromagnetic to ferromagnetic phase transition [1], spin excitation with the inverse Faraday effect [2], ultrafast spin reorientation as a result of optical excitation [3], inverse Faraday effect assisted domain selection in heat induced spin reorientation [4], and heat induced magnetization reversal [5]. Spin excitation with the inverse Faraday effect is one of the major mechanisms of ultrafast spin excitation, where its importance in orthoferrites has been discussed by Kimel *et al.* [2]. Its dynamics is simple, because it is regarded as an impulsive transfer of angular momentum to a spin system. In contrast, the heat mechanism, which is important in memory device applications, is complicated, because it may involve several steps, i.e., electronic transition, relaxation of the excited state via phonon emission, and finally resulting in modulation of the spin system. The aim of this paper is to clarify the dynamics of this process in picosecond time scale.

One method to observe the real-time spin ordering dynamics is to use a terahertz (THz) pulse [6–9]. When the THz pulse enters a magnetically ordered sample, a magnetic moment in the sample experiences a force which equals the cross product of the magnetic moment and the THz magnetic field. This force tilts the magnetic moment out of equilibrium. After being tilted, the magnetic moment starts to precess around the internal effective magnetic field, which defines easy axis of the crystal. This method induces spin precession without causing unwanted electronic excitation and heat. Thus, photothermally

excited spin dynamics can be clearly probed with the THz induced spin precession in a real-time scale.

In this paper we utilized THz pulse induced spin precession to monitor the dynamics of the anisotropy parameter, which is modified by photoexcitation in the antiferromagnetic spin systems ErFeO_3 and DyFeO_3 . The experiment revealed a slow frequency shift of the antiferromagnetic resonance subsequent to the optical excitation. This gradual change was attributed to the slow energy transfer from the Fe^{3+} $3d$ electron system to the rare-earth $4f$ electron system, which in turn alters the anisotropy of the Fe^{3+} spins.

Orthoferrites belong to the class of a weak ferromagnet where antiferromagnetic Fe^{3+} ions cant slightly, giving rise to a weak macroscopic magnetization [10]. Figure 1(a) shows the spin configurations of Fe^{3+} in ErFeO_3 and DyFeO_3 for the temperature range studied here. Although there are four Fe^{3+} ion sublattices in a unit cell, the commonly used two-sublattice approximation is known to yield reasonably accurate results [11–13]. In the two-sublattice model, the Hamiltonian of the Fe^{3+} spins \mathbf{s}_1 and \mathbf{s}_2 is given by

$$H = 2JZ\mathbf{s}_1 \cdot \mathbf{s}_2 + D(s_{1x}s_{2z} - s_{1z}s_{2x}) - A_x(s_{1x}^2 + s_{2x}^2) - A_y(s_{1y}^2 + s_{2y}^2) - A_z(s_{1z}^2 + s_{2z}^2), \quad (1)$$

where J , Z , D , and A , respectively, represents exchange parameter, number of the nearest neighbor spins, Dzyaloshinskii parameter, and anisotropy parameters [12,13]. The equations of motion for \mathbf{s}_1 and \mathbf{s}_2 are obtained by

$$\dot{\mathbf{s}}_i = -i[\mathbf{s}_i, H]. \quad (2)$$

Taking the x axis as the easy axis ($s_{1x} = 1$, $s_{2x} = -1$) and solving the equation of motion for s_{iy} and s_{iz} , two different modes of oscillations with different resonant frequencies

$$\omega_F \propto 2\sqrt{12J|A_x - A_z|} \quad (3)$$

and

$$\omega_{AF} \propto 2\sqrt{12J|A_x - A_y|} \quad (4)$$

are obtained. Here, since $s_{iy} \ll s_{ix}$, and $s_{iz} \ll s_{ix}$, second order terms of s_{iy} and s_{iz} , were ignored, and this approximation

*Present address: Hitachi Ltd., Yokohama 244-0817, Japan.

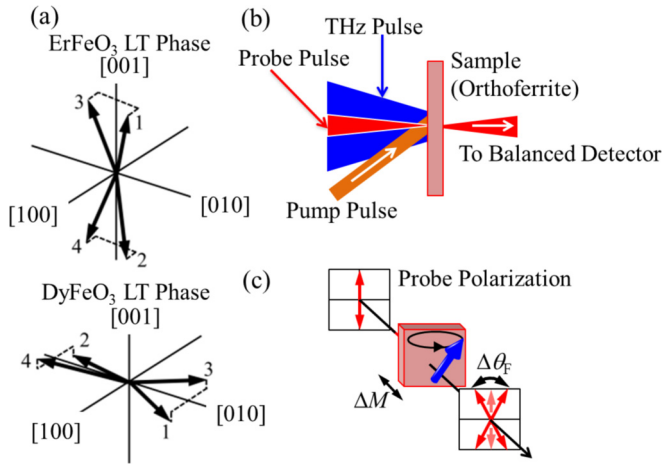


FIG. 1. (Color online) (a) Spin configurations of Fe^{3+} spins in ErFeO_3 and DyFeO_3 for the temperature range observed in this study. [100], [010], and [001] correspond to crystallographic axes. (b) Illustration showing the experimental configuration of the incident THz pulse, probe pulse, pumping pulse, and orthoferrite sample. (c) The relation between the spin precession and the observed Faraday rotation of the probe pulse. The change in the Faraday rotation $\Delta\theta_F$ reflects the fluctuation of magnetization ΔM_z along the thickness direction (z axis in the figure) of the sample.

eliminates terms including the Dzyaloshinskii parameter D . Also, because $A \ll J$, terms on the order of A^2 were dropped. The resonance modes with frequencies ω_F and ω_{AF} are often named as quasiferromagnetic (F) mode and quasiantiferromagnetic (AF) mode, respectively. F mode is a precession of the weak magnetization and can be excited with a THz magnetic pulse perpendicular to the weak magnetization. AF mode on the other hand can be viewed as the magnitude fluctuation of the weak magnetization and this mode is excited by a THz magnetic pulse along the weak magnetization [14,15].

Equations (3) and (4) state that changes in the anisotropy parameters lead to frequency shift. Such shifts in the resonant frequency are actually observed in some orthoferrites where rare-earth ions are paramagnetic. The paramagnetic moment in these types of rare-earth ions increases when the temperature is lowered. This affects the anisotropy parameters of the Fe^{3+} ions and leads to switching of the Fe^{3+} spin easy axes. This switching is known as the spin reorientation transition [16,17]. The samples used in this report, ErFeO_3 and DyFeO_3 , are both known to exhibit such transition ($T_{\text{SRPT}} = 87 - 96$ K for Er and 40 K for Dy [16]). The low temperature phases shown in Fig. 1(a) are studied here.

In the visible and near infrared (NIR) spectral regions, orthoferrites have absorption peaks due to the d -electron transitions ${}^6A_1 \rightarrow {}^4T_1$ and ${}^6A_1 \rightarrow {}^4T_2$ of Fe^{3+} in an octahedral crystal field [18]. According to the past reports, soon after the absorption of optical pulse, Fe^{3+} electrons equilibrate with the lattice. Subsequently, the excited lattice interacts with the rare-earth ion and $4f$ electrons are redistributed within the sublevels [3]. This electronic excitation in the rare-earth ion is expected to affect the spin precession frequency through anisotropy change.

We used the three-pulse configuration with THz pump, NIR pump, and NIR Faraday probe. The laser pulse for THz generation, NIR pump, and NIR Faraday probe are provided by a femtosecond Ti:sapphire laser source (1 kHz repetition regenerative amplifier, $\lambda = 800$ nm, and 100 fs pulse width). As Fig. 1(b) shows, the THz induced spin excitation is observed by transmitting the linearly polarized NIR ($30 \mu\text{m}$ spot diameter) probe pulse through the sample. Magnitude fluctuation of the magnetization along the thickness direction of the sample is detectable through Faraday rotation of the probe pulse. When the precession of spins cause magnitude fluctuation along this direction, the precession is observed as an oscillation of Faraday rotation angle [Fig. 1(c)]. The transmitted probe pulse goes through a $\lambda/2$ waveplate and a Wollaston prism, and the polarization change is balance detected by a pair of photodiodes.

The incident THz pulse was generated from the LiNbO_3 crystal pumped with a pulse front tilted femtosecond laser. The THz pulse was focused to $300 \mu\text{m}$ diameter, and the peak electric field strength of the THz pulse was roughly 200 kV/cm .

To see the influence of the NIR pumping, a linearly polarized pump pulse (100 mJ/cm^2 per pulse) irradiated the sample [Fig. 1(b)]. Accumulation of the pump pulse induced heat was avoided by minimizing the spot diameter of the pump pulse ($100 \mu\text{m}$). Since this is larger than the spot diameter of the probe pulse, the pump fluence inside the observed sample area is regarded as homogeneous.

Figure 2 (upper curve) shows the result of the transient Faraday rotation observed with a $100 \mu\text{m}$ thick (001)-cut ErFeO_3 sample at 30 K (low temperature phase). The time origin of this figure is defined as the time when the THz peak arrives at the sample. This time origin is calibrated by the EO sampling where the GaP crystal is placed instead of the sample. THz magnetic field parallel to the [010] axis excited the

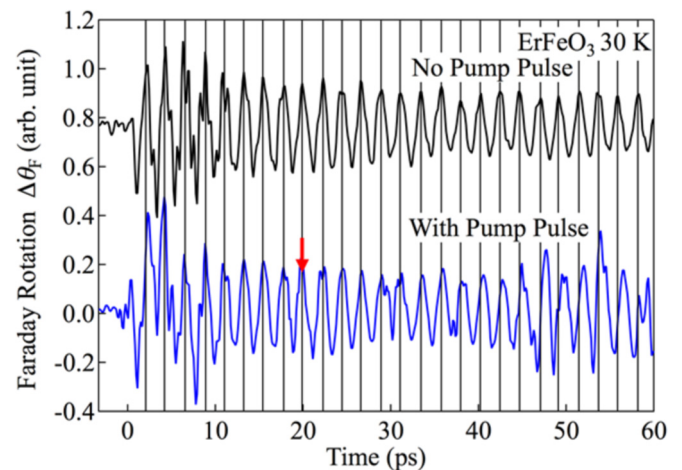


FIG. 2. (Color online) Time dependent Faraday rotation signals induced by the THz excited coherent spin precession in ErFeO_3 at 30 K. The THz pulse arrives at the sample at $t = 0$ ps. The waveform on the upper side is obtained with no additional pumping pulse. The waveform on the bottom was obtained with an additional 100 mJ/cm^2 fluence NIR pumping pulse. The arrow denotes the timing the pumping laser arrived at the sample.

F mode, which is a precession of the weak magnetization inside the (100) plane. This precession is detected with the Faraday rotation of the probe pulse. As described in this figure, the THz pulse arriving at $t = 0$ ps initiates monochromatic oscillation with a frequency of approximately 450 GHz. This matches with the F mode resonant frequency at $T = 30$ K [7,11].

Figure 2 (lower curve) also shows the time dependent Faraday rotation signal with the pump pulse arriving at $t = 20$ ps. Irradiation of the pump pulse does not deteriorate the THz induced coherent F mode precession, which enables the influence of the pump pulse to be probed through the spin precession. Close comparison of the two waveforms in Fig. 2 shows that the phases of the precession in the two cases are identical prior to the pumping at $t = 20$ ps. However, after the pumping, the phase of the oscillation starts to deviate from each other, and the phase shift begins to become prominent at around $t = 35$ ps. The readers may notice that the oscillation amplitude in the figures do not decay monotonously. This behavior was observed particularly in the low temperature phase of the ErFeO_3 . Because analysis on the origin of such behavior is outside the scope of this report, details will be reported elsewhere.

For more precise analysis of the data, time-frequency analysis was performed. Figures 3(a) and 3(b) show the time-frequency mapping of the temporal waveforms in Fig. 2 obtained from the Choi-Williams transformation which provides higher resolution of frequency and time, compared to methods such as wavelet transformation and short time Fourier transform [19,20]. The two time-frequency plots show obvious differences. When no pump pulse is irradiated, the F mode

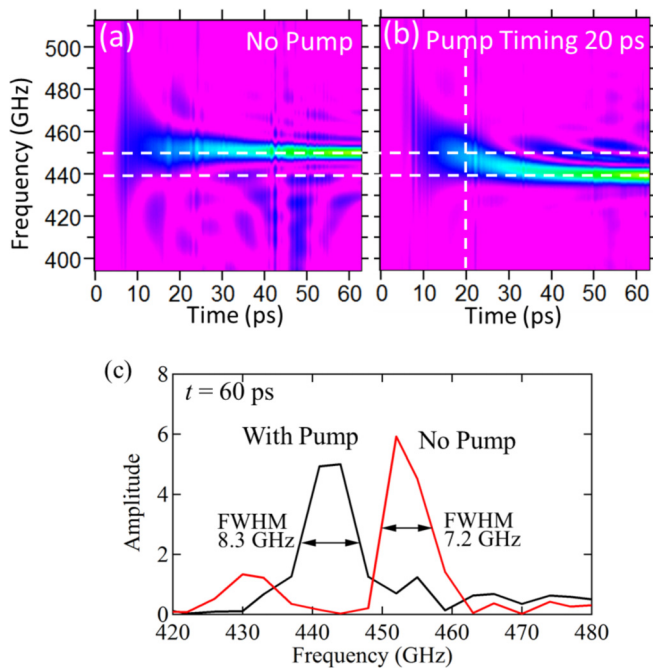


FIG. 3. (Color online) Time-frequency mappings of the time dependent Faraday rotation signals in ErFeO_3 at 30 K computed from the waveforms in Fig. 2 with (a) no additional pumping pulse and (b) with 100 mJ/cm^2 pumping pulse arriving at $t = 20$ ps. (c) Faraday rotation spectra at $t = 60$ ps obtained from the cross section of the time-frequency mappings (a) and (b).

resonant frequency is independent of time [Fig. 3(a)]. On the other hand, when the pump pulse is irradiated, the frequency gradually changes [Fig. 3(b)]. This gradual change amounts to approximately 10 GHz. The frequency continues to shift for more than 10 ps after the pumping. The spectra in Fig. 3(c) shows the $t = 60$ ps cross sections of the mappings in Figs. 3(a) and 3(b). Because the observed frequency shift is greater than the FWHM of the spectra (8.3 and 7.2 GHz), we judged that the frequency shift is statistically significant. Thus, the above-mentioned phase shift corresponds to this frequency shift.

As Eqs. (3) and (4) show, the resonant frequencies depend on the exchange constant and anisotropy parameters. Therefore, the observed frequency shift is attributed to changes in these parameters. For the following reason we exclude the exchange parameter as the cause for the observed frequency shift. The majority of the absorbed pump pulse energy with $\lambda = 800$ nm is used for exciting the $3d$ electrons in Fe^{3+} ions [18]. Since the exchange interaction takes place inside the covalently bound Fe-O-Fe unit, the exchange parameter J is expected to respond instantaneously when the $3d$ electrons are excited. However, this contradicts with the observed gradual frequency shift of the precession.

On the other hand, the time scale of the frequency shift matches with that of the energy transfer from Fe^{3+} $3d$ electrons to Er^{3+} $4f$ electrons. According to Ref. [3], strong electron-phonon coupling transfers the energy from Fe^{3+} electrons to the lattice within 500 fs. After that, the energy is passed on to the Er^{3+} electrons. A weak electron-phonon coupling of the Er^{3+} $4f$ electrons compared with that of the Fe^{3+} $3d$ electrons [21] results in a longer time constant of about 15 ps [3], which is close to the observed frequency shift. Excitation of Er^{3+} $4f$ electrons alters the distribution of the electrons within the crystal field split sublevels which consequently changes the paramagnetic moment of the Er^{3+} ions. In fact, as we have mentioned previously, the anisotropic parameters of the Fe^{3+} spins in the orthoferrites are known to be dependent on the paramagnetic moment of the Er^{3+} ions [17,18]. Therefore, it is natural to assume that redistribution of $4f$ electrons in Er^{3+} leads to a frequency shift of the Fe^{3+} spin precessions. Thus, the observed precession frequency change is attributed to the change in the anisotropic parameter A .

Using the relation between the resonant frequency and the anisotropic constant shown in Eq. (3), the measured frequency shift is converted into the change in the anisotropic parameter $|A_x - A_z|$ [Fig. 4(a)]. It can be seen that the photoinduced electronic excitation decreases the anisotropy parameter $|A_x - A_z|$. As described in the figure, the gradual change of anisotropy can be fitted with $A(t) = (A_{\text{Final}} - A_{\text{Initial}}) \exp(-t/\tau)$. The result of fitting shows that the time constant is $\tau = 11$ ps, which is very close to the energy transfer time constant from the lattice to the Er^{3+} $4f$ electrons [3]. At around 30 K, a temperature increase results in a decrease of the F mode frequency [Fig. 4(b)]. Considering Eq. (3), this temperature dependence indicates that excitation of the Er^{3+} electrons leads to a decrease of anisotropic parameter $|A_x - A_z|$. This behavior agrees with the observed anisotropy change induced by the femtosecond pulse laser excitation.

With the pump-probe experiment at 5 K, similar behavior of the Er^{3+} electron was observed [Fig. 5(a)]. Here the time

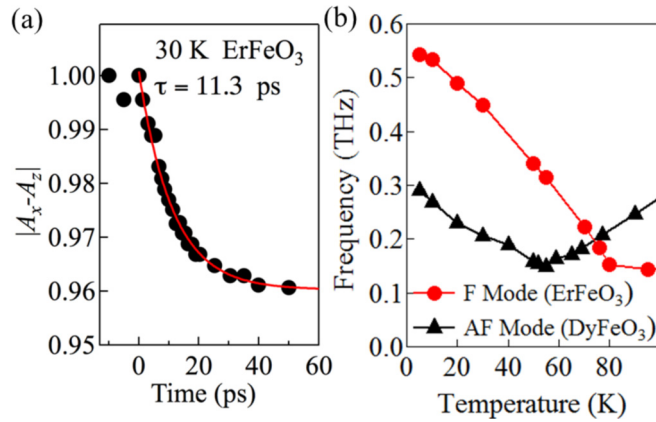


FIG. 4. (Color online) (a) The time dependent anisotropy change in ErFeO₃ at 30 K converted from the frequency shift shown in Fig. 3(b). The pumping pulse arrives at the sample at $t = 0$ ps. The measured anisotropy is normalized with the anisotropy at $t = 0$ ps. The solid line shows the result of curve fitting. (b) Temperature dependence of F mode resonant frequency in ErFeO₃ and AF mode resonant frequency in DyFeO₃.

constant was about 20 ps, and it was found that the energy transfer between the Fe³⁺ electrons to Er³⁺ electrons is slowed in lower temperature.

A similar experiment was also conducted on a DyFeO₃ single crystal. Comparing the temperature dependence of the

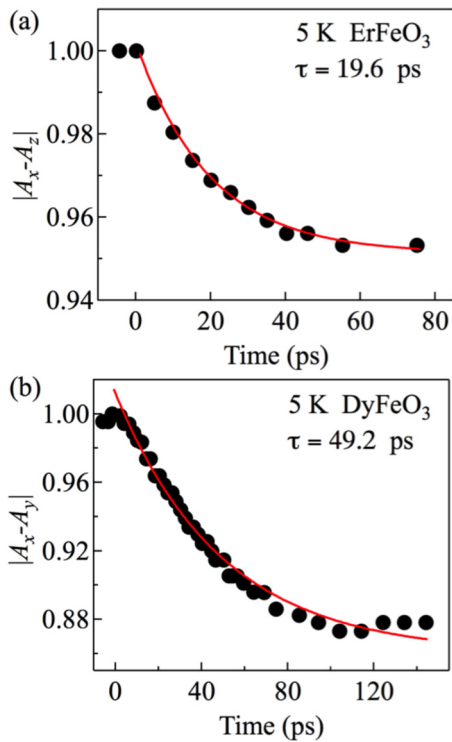


FIG. 5. (Color online) The photoexcited time dependent anisotropy change observed via spin precession frequency shift at 5 K in (a) ErFeO₃ and (b) DyFeO₃. The pump pulse with 100 mJ/cm² fluence arrives at the sample at 0 ps. The values are normalized with the anisotropy at $t = 0$ ps. Solid lines show the fitting result.

magnetic resonance modes in Fig. 4(b) with Eqs. (3) and (4), it is noticed that excitation of the rare-earth 4*f* electrons in the low temperature phase tends to decrease $|A_x - A_z|$ in ErFeO₃, while $|A_x - A_y|$ relevant to ω_{AF} is decreased in DyFeO₃. The marked difference between ErFeO₃ and DyFeO₃ is due to the difference in the single ion anisotropy of the Er³⁺ and Dy³⁺ paramagnetic moment [17]. One can notice that the temperature dependence of the AF mode frequency of DyFeO₃ shows a bending at about 55 K [triangles in Fig. 4(b)]. At this temperature $A_x = A_y$, and the easy axis of the Fe³⁺ spins turns to the [100] direction above this temperature. The mismatch with the transition temperature of 40 K in the literature [16] can be explained by a strong dependence of the transition temperature to an external magnetic field. Our THz measurement with an external magnetic field applied along the [001] axis revealed a transition temperature decrease of 0.46 K per 0.1 T. In the past magnetostatic researches, application of the external magnetic field was inevitably used, and this may have resulted in underestimation of the transition temperature.

Redistribution of 4*f* Dy³⁺ electrons within the sublevels is expected to modulate the AF mode frequency via an anisotropy parameter, which can be detected as a frequency shift reflecting the slope of the frequency vs temperature curve in Fig. 4(b). Thus, the AF mode in DyFeO₃ was selected as a probe for monitoring the effect of the pump pulse. In order to excite the AF mode with the THz pulse and observe the AF mode motion with the Faraday rotation, the (101) sample with 100 μ m thickness was prepared. The incident THz magnetic field was polarized along the [10 $\bar{1}$] direction of the sample. The result of this measurement is shown in Fig. 5(b). Similar to the case of ErFeO₃, photoinduced picosecond time scale anisotropy change was observed through the resonant frequency shift. The time constant for reaching the equilibrium was 50 ps, much longer than the time constant observed in ErFeO₃. This result indicates that the electron-phonon coupling of the Dy³⁺ 4*f* electrons is much weaker than that of Er³⁺ electrons. The work reported in the past shows that the lanthanide-ion series (La, Ce, Pr, Nd, Pm, Sm, Eu, Gd, Tb, Dy, Ho, Er, Tm, Yb, and Lu, arranged in ascending order of the amount of 4*f* electron it contains) have stronger electron-phonon coupling at the both ends of the series (La, Ce, Yb, and Lu). As the number of the 4*f* electrons approaches 7, that is Gd, the electron-phonon coupling decreases [21]. Since Dy³⁺ is closer to the center of the series compared to Er³⁺, electron-phonon coupling is weaker in the Dy³⁺ 4*f* electron system, which agrees with our present result. This agreement supports the interpretation that energy transfer through electron-phonon coupling of the rare-earth 4*f* electron system plays a vital role in photoinduced spin excitation dynamics studied here.

In conclusion, by using the precession frequency as a probe of the magnetic anisotropy experienced by Fe³⁺ ions, the dynamics of the laser induced change of spin ordering was continuously tracked. Clear evidences supporting the picture of the spin modification starting from the electronic excitation in Fe³⁺ were obtained. It was shown that the weak electron-lattice coupling of the rare-earth ion is the bottleneck of this process. These results enable deeper understanding of the photothermally excited ultrafast spin dynamics. In addition, the method

presented here offers a possibility to explore the ultrafast spin dynamics with a time resolution less than the precession period and it is expected to promote more thorough and extensive researches on spin orientation dynamics triggered by electronic excitation.

This work has been supported by JSPS KAKENHI Grant-in-Aid (Grants No. 23244063, No. 26287060, No. 25286063, No. 26600109, and No. 11J02179) and Research Foundation for Opto-Science and Technology. K.Y. is grateful for the support from the JSPS Research Fellowship.

-
- [1] T. Li, A. Patz, L. Mouchliadis, J. Yan, T. A. Lograsso, I. E. Perakis, and J. Wang, Femtosecond switching of magnetism via strongly correlated spin-charge quantum excitations, *Nature (London)* **496**, 69 (2013).
- [2] A. V. Kimel, A. Kirilyuk, F. Hansteen, R. V. Pisarev, and Th. Rasing, Nonthermal optical control of magnetism and ultrafast laser-induced spin dynamics in solids, *J. Phys. Condens. Matter* **19**, 043201 (2007).
- [3] J. A. de Jong, A. V. Kimel, R. V. Pisarev, A. Kirilyuk, and Th. Rasing, Laser-induced ultrafast spin dynamics in ErFeO_3 , *Phys. Rev. B* **84**, 104421 (2011).
- [4] J. A. de Jong, I. Razdolski, A. M. Kalashnikova, R. V. Pisarev, A. M. Balbashov, A. Kirilyuk, Th. Rasing, and A. V. Kimel, Coherent control of the route of an ultrafast magnetic phase transition via low-amplitude spin precession, *Phys. Rev. Lett.* **108**, 157601 (2012).
- [5] T. A. Ostler *et al.*, Ultrafast heating as a sufficient stimulus for magnetization reversal in a ferrimagnet, *Nat. Commun.* **3**, 666 (2012).
- [6] K. Yamaguchi, M. Nakajima, and T. Suemoto, Coherent control of spin precession motion with impulsive magnetic fields of half-cycle terahertz radiation, *Phys. Rev. Lett.* **105**, 237201 (2010).
- [7] K. Yamaguchi, T. Kurihara, Y. Minami, M. Nakajima, and T. Suemoto, Terahertz time-domain observation of spin reorientation in orthoferrite ErFeO_3 through magnetic free induction decay, *Phys. Rev. Lett.* **110**, 137204 (2013).
- [8] M. Nakajima, A. Namai, S. Ohkoshi, and T. Suemoto, Ultrafast time domain demonstration of bulk magnetization precession at zero magnetic field ferromagnetic resonance induced by terahertz magnetic field, *Opt. Express* **18**, 18260 (2010).
- [9] T. Kampfrath, A. Sell, G. Klatt, A. Pashkin, S. Mährlein, T. Dekorsy, M. Wolf, M. Fiebig, A. Leitenstorfer, and R. Huber, Coherent terahertz control of antiferromagnetic spin waves, *Nat. Photon.* **5**, 31 (2011).
- [10] A. K. Zvezdin and V. A. Kotov, *Modern Magneto-optics and Magneto-optical Materials* (Institute of Physics, Bristol, 1997).
- [11] G. V. Kozlov, S. P. Lebedev, A. A. Mukhin, A. S. Prokhorov, I. V. Fedorov, A. M. Balbashov, and I. Y. Parsegov, Submillimeter backward-wave oscillator spectroscopy of the rare-earth orthoferrites, *IEEE Trans. Magn.* **29**, 3443 (1993).
- [12] C. H. Tsang, R. L. White, and R. M. White, Spin-wave damping of domain walls in YFeO_3 , *J. Appl. Phys.* **49**, 6063 (1978).
- [13] N. Koshizuka and K. Hayashi, Raman Scattering from Magnon Excitations in RFeO_3 , *J. Phys. Soc. Jpn.* **57**, 4418 (1988).
- [14] G. F. Herrmann, Magnetic resonances and susceptibility in orthoferrites, *Phys. Rev.* **133**, A1334 (1964).
- [15] A. A. Mukhin, M. Biberacher, A. Pimenov, and A. Loidl, Antiferromagnetic resonances and magnetization of a canted antiferromagnet, *J. Magn. Reson.* **170**, 8 (2004).
- [16] R. L. White, Review of recent work on the magnetic and spectroscopic properties of the rare-earth orthoferrites, *J. Appl. Phys.* **40**, 1061 (1969).
- [17] T. Yamaguchi, Theory of spin reorientation in rare-earth orthochromites and orthoferrites, *J. Phys. Chem. Solids* **35**, 479 (1974).
- [18] D. L. Wood, J. P. Remeika, and E. D. Kolb, Optical spectra of rare-earth orthoferrites, *J. Appl. Phys.* **41**, 5315 (1970).
- [19] L. Cohen, Time-frequency distributions—a review, *Proc. IEEE* **77**, 941 (1989).
- [20] H. Choi and W. J. Williams, Improved time-frequency representation of multicomponent signals using exponential kernels, *IEEE Trans. Acoust. Speech. Signal Process.* **37**, 862 (1989).
- [21] A. Ellens, H. Andres, M. L. H. ter Heerdt, R. T. Wegh, A. Meijerink, and G. Blasse, Spectral-line-broadening study of the trivalent lanthanide-ion series. II. The variation of the electron-phonon coupling strength through the series, *Phys. Rev. B* **55**, 180 (1997).